

HARNESSING THE POWER OF AI BASED IMAGE GENERATION MODEL DALL·E 2 IN AGRICULTURAL SETTINGS *

Ranjan Sapkota

Center for Precision & Automated Agricultural Systems
Department of Biological Systems Engineering, Washington State University, USA
ranjan.sapkota@wsu.edu

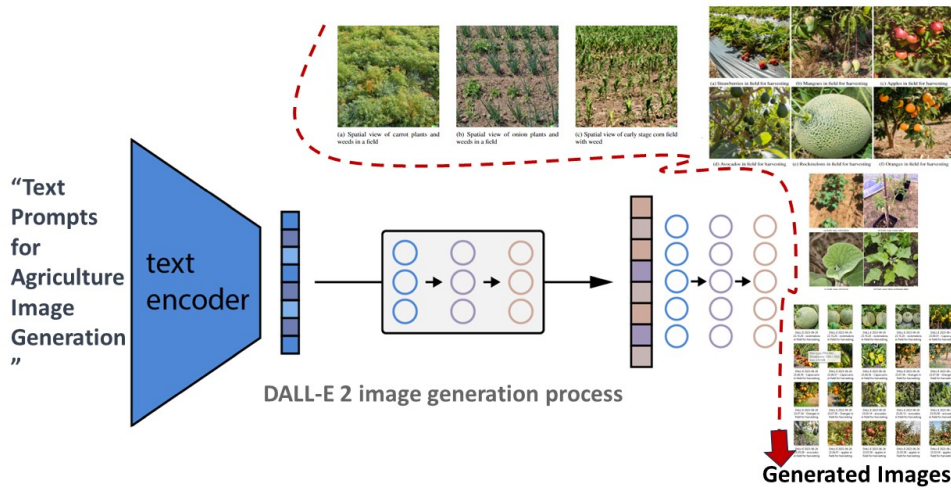


Figure 1: A modified birds-eye view of the DALL-E 2 image generation process in Agricultural Settings, showcasing the transformation of text prompts into agriculture-specific images for research and analysis.

ABSTRACT

This study investigates the potential impact of artificial intelligence (AI) on the enhancement of visualization processes in the agricultural sector, using the advanced AI image generator, DALL-E 2, developed by OpenAI. By synergistically utilizing the natural language processing proficiency of chatGPT and the generative prowess of the DALL-E 2 model, which employs a Generative Adversarial Networks (GANs) framework, our research offers an innovative method to transform textual descriptors into realistic visual content. Our rigorously assembled datasets include a broad spectrum of agricultural elements such as fruits, plants, and scenarios differentiating crops from weeds, maintained for AI-generated versus original images. The quality and accuracy of the AI-generated images were evaluated via established metrics including mean squared error (MSE), peak signal-to-noise ratio (PSNR), and feature similarity index (FSIM). The results underline the significant role of the DALL-E 2 model in enhancing visualization processes in agriculture, aiding in more informed decision-making, and improving resource distribution. The outcomes of this research highlight the imminent rise of an AI-led transformation in the realm of precision agriculture.

Keywords generative adversarial network (GAN) · chatGPT · DALL·E2 · GPT4 · Deep Learning · machine learning · precision agriculture

**Arxiv*: A survey analysis

1 Introduction

Synthetic images are artificial visuals created by computer algorithms, often designed to resemble real-world entities or scenarios [1]. Their significance lies in their application potential and versatility, providing realistic visual representations for diverse fields, aiding in data analysis, decision-making, and driving innovative solutions [2]. The utility of synthetic images has been already recognized across numerous fields in recent years such as Healthcare [3, 4], biomedicine [5] Fashion industry [6, 7], Architecture and Interior Design [8] Geospatial studies [9, 10], Automotive Industry [11], Security and Surveillance [12, 13] and so on.

In the past, researchers have implemented varieties of traditional methods for creating synthetic images. An example of such an approach is parametric methods which involve the use of mathematical equations and parameters to create images. For instance, Chen et al. [14] made use of Bézier Curves to create synthetic non-ellipsoidal cell nuclei microscopy images, overcoming the limitations of traditional spherical and ellipsoidal models, which, when used for training a modified 3D U-Net deep learning model, resulted in more accurate segmentation in volumes with irregularly shaped nuclei. Likewise, Alberto et al. [15] recently presented a method to design mechanical metamaterials with complex lattice structures through the use of parameterizing through Bézier Curves. Another conventional synthetic image generation method is through ray tracing, which is a computational technique used in computer graphics to generate an image by tracing the path of light as pixels in an image plane and simulating the effects of its encounters with virtual objects[16]. For example [17] utilized a genetic evolution search strategy, which expedites the search for optimal matching blocks, improving the speed and quality of synthetic image generation, an approach distinct from the conventional ray tracing method. Additional study on ray tracing based synthetic image generation by Ben et al. [18] enhanced the Neural Radiance Fields (NeRF) technique for high-quality view synthesis by training it on raw, unprocessed images rather than the traditional tonemapped low dynamic range (LDR) images, enabling manipulation of focus, exposure, and tonemapping post-rendering, and achieving superior scene reconstruction even from extremely noisy low-light images. Likewise, another approach of generating synthetic image is through Physically Based Rendering (PBR), which is an approach in computer graphics that seeks to render images in a way that models the flow of light in the real world [19]. Recently, Hodaň et al. [20] created a method for synthesizing highly photorealistic images of 3D object models using realistic scenes, physics simulations, and physically based rendering, which were then used to train a convolutional neural network, resulting in significant improvements in object detection performance and marking a step towards training object detectors without the need for real or annotated images.

However these traditional models of synthetic image generation, including parametric methods, ray tracing, and Physically Based Rendering (PBR), although instrumental in advancing various fields, possess several limitations. Firstly, parametric models often depend heavily on the precision and accuracy of the defined parameters and mathematical equations [21, 22]. This rigidity makes it challenging to adapt these models to more complex, irregular shapes or scenarios that defy the predefined mathematical structures [23]. Furthermore, ray tracing, despite producing high-quality, realistic images, is computationally intensive and time-consuming, posing a significant barrier for real-time applications or scenarios where rapid image generation is crucial [24]. In addition, it struggles with simulating global illumination effects like indirect light, caustics, or interreflections [25]. Physically Based Rendering (PBR) strives for realism by closely modeling light physics, but this commitment to realism can also limit its flexibility [26, 27] making the assumptions and simplifications in PBR not accurate to represent all real-world scenarios and achieving the desired level of photorealism often requires a great deal of computational resources and time.

Generative Adversarial Networks (GANs) [28] can be particularly beneficial for synthetic image generation, offering distinct advantages over traditional methods such as parametric methods, ray tracing, and Physically Based Rendering (PBR) [29]. GANs leverage the power of two competing neural networks – the generator and the discriminator – to produce realistic synthetic images [30]. Unlike parametric models that are rigid and limited by predefined mathematical structures, GANs offer flexibility by learning the complex, high-dimensional distributions of real-world data, enabling them to generate images that better resemble reality, even in complex and irregular scenarios [31]. This learning-based approach also solves the problem of intensive computational demands associated with methods like ray tracing, as once trained, GANs can generate new images in a fraction of the time [24, 25, 27]. Moreover, GANs overcome the realism-flexibility trade-off seen in PBR [32]. They not only capture the intricate details and nuances that contribute to the realism of images, but also allow for manipulations, offering control over the generation process without sacrificing the quality or realism of the output. Furthermore, GANs are not limited to reproducing existing data - they can generate entirely new, yet plausible images [33], unlocking creative potential in a variety of applications.

Recent research has explored the use of Generative Adversarial Networks (GANs) in agriculture, particularly in disease detection [34, 35], data augmentation [34, 36], and image translation [36, 37], demonstrating impressive outcomes. Abbas et al. [38] employed a Conditional GAN (C-GAN) to generate synthetic images of tomato plant leaves, which, coupled with a DenseNet121 model and transfer learning, achieved a high accuracy of up to 99.51% in tomato leaf disease classification. Similarly, Barth et al. [39] optimised the realism of synthetic agricultural images using cycle

GANs, which translated synthetic images to empirical ones, resulting in a more authentic color distribution and improved image features, thereby bridging the gap between synthetic and empirical data. Lu et al. [40] took a unique approach by using GANs to synthesize insect pest training images, effectively augmenting limited datasets and enhancing the performance of insect pest convolutional neural network classifiers, which led to an F1-score of 0.95. Nazki et al. [41] proposed a novel synthetic sampling solution to overcome the challenges of small and imbalanced datasets, utilizing GANs for image-to-image translation in plant disease datasets, thereby shifting the classification decision boundary for more accurate results. Lastly, another study by Barth et al. [42] provided evidence of the potential for domain adaptation to translate and improve synthetic data to the real empirical domain, resulting in improved segmentation learning and reduced dependency on manually annotated data. Overall, the application of GANs in agriculture signifies a promising direction for achieving more precise and efficient results in disease detection and image analysis, while also addressing data limitations. Table 1 provides a comprehensive summary of the research that have been performed in the last 5 years that investigated the use of synthetic image generation in agriculture using GANs :

Reference	Target Crop	Synthetic Image Generation Technique	Primary Applications
[38]	Tomato plant leaves	C-GAN	Disease detection
[43]	Tea leaf	C-DCGAN	Disease detection
[44]	Charlock, Cleavers, Common Chickweed, Fat Hen, Maize, Scentless Mayweed, Shepherd's Purse, Small-flowered Cranesbill, and Sugar Beets	Wac-GAN	Multiple species plant seedlings
[45]	Orchid seedlings	C-DCGAN	Plant Vigor rating
[46]	Wheat	CycleGAN	Plant head detection
[47]	Lemons	C-GAN	Fruit quality assessment and defect classification
[48]	Maize plants	TasselGAN (DCGAN)	Image generation of maize tassels against sky backgrounds
[49]	Jujubes	DCGAN	Quality grading
[50]	Arabidopsis thaliana and cauliflower plants	CGAN (Pix2Pix)	Laboratory-grown and field-grown image generation
[51]	Grapevine Berries	CGAN/CDCGAN	Estimation of occluded fruits
[52]	Kiwifruit	CGAN	Filling in missing fruit surface (Reconstruction)
[53]	Apple orchard	CycleGAN	Unseen fruits counting
[54]	Sugar beet, sunflower	CGAN/CDCGAN	Crop/weed segmentation in precision farming
[55]	Citrus	DCGAN	Disease severity detection
[56]	Blueberry leaves	DCGAN	Fruit tree disease classification
[57]	Apple canopy	CycleGAN	Disease detection
[58]	Cucumber leaves	CycleGAN	Plant disease diagnosis
[59]	Wheat	SR-GAN	Wheat stripe(yellow) rust classification
[60]	Grape, Orange, Potato, Squash, Tomato	WGAN-GP	Plant disease classification
[61]	Apple, Corn, Grape, Potato, Tomato	DoubleGAN	Plant disease detection
[62]	Apple, corn, tomato, potato	Reinforced GAN	Leaf disease detection

Table 1: Summary of synthetic image generation techniques through generative Adversarial Networks (GANs) in agricultural research in the last 5 years. The table lists the references, target crops, the image generation techniques utilized, and the primary applications or achievements of the studies.

The utilization of Generative Adversarial Networks (GANs) in agricultural image analysis, as explored in several recent studies, represents an effective approach to improving model performance in visual recognition tasks, such as image classification, segmentation, object detection, and localization [36]. The application of GANs, as evidenced in the studies [38, 39, 5, 40, 41, 34, 35, 34, 36, 40] has achieved significant strides in addressing issues of biological variability and unstructured environments. The incorporation of GANs into the agricultural sector, as demonstrated in a series of recent investigations, has ushered in an innovative and efficient way to bolster model performance in tasks pertaining to visual recognition. These tasks, encompassing image classification, segmentation, object detection, and localization, are critical to agriculture. However, these models often grapple with challenges stemming from biological variability and unstructured environments [63]. As illustrated in the several studies above, the application of GANs

has made remarkable progress in tackling these issues, through means such as generating synthetic images of tomato leaves for disease detection, optimizing the realism of synthetic agricultural images, synthesizing insect pest training images, and improving data distribution learning in cases of limited and imbalanced datasets. These applications not only underscore the potential of GANs to enhance model performance but also alleviate the laborious process of image collection for vast majority of agricultural crops [64].

However, the necessity for an even more robust and advanced solution in image generation is palpable and it is worth noting that the journey with GANs is still in progress, and many challenges and opportunities await exploration. The groundbreaking DALL·E 2, developed by OpenAI (OpenAI, California, USA), has taken the realm of AI-based image generation to unprecedented heights. It takes advantage of a powerful blend of technologies, including Compact Language-Image Pretrained (CLIP) embeddings, Principal Component Analysis (PCA) dimensionality reduction, and of course, Generative Adversarial Networks (GANs), resulting in a model that surpasses traditional image generation methods. The brilliance of DALL·E 2 lies in its unique capability to convert textual descriptions into visually accurate and diverse images. This attribute originates from its text-conditional hierarchical image generation strategy. Impressively, this model has undergone training on an extensive variety of image-text pairs, much like its sibling model, ChatGPT, which has been trained on enormous text corpora. Both models, stemming from the same OpenAI lineage, manifest exceptional competence in managing intricate, multi-dimensional tasks. For instance, while ChatGPT excels at generating contextually relevant textual responses, DALL·E 2 emerges as a powerhouse in producing images that accurately mirror the semantics of the input text. In essence, the advent of DALL·E 2, akin to the impact of ChatGPT, signals a significant advancement in the AI domain, challenging the existing norms and opening avenues for innovative applications across various sectors by converting the textual descriptions into realistic visuals showing the potential to revamp a range of agricultural processes and practices. Although the process of synthetic image generation has moved from a complex expertise skill requirement to simple production, yet, to harvest the full advantage of this AI-driven transformation, it is imperative to rigorously examine the practicality and effectiveness of AI-synthesized images, specifically in the context of their realism and applicability in agriculture. Additionally, the recent adoption of Dall.E 2 model in wide range of applications such as healthcare, automotive, security and surveillance, fashion, construction, architecture and design, [65]. This make it urge need in adoption and exploration of the AI based image generation model DALL.E 2 in agricultural settings. With this backdrop, this study sets the following objectives:

- To explore the capabilities of DALL·E 2's AI-generated images in the realm of agricultural applications, with an emphasis on fruits, plants, and crop versus weed scenarios. The focus is to assess their realism, utility, and broader implications in the field.
- To evaluate the impact of DALL·E 2 on agricultural visualization by computing the feature similarity and noises in the AI generated and original images.

2 Methods

2.1 Data collection and compilation

To ensure a broad spectrum of the agricultural domain, the dataset in this study were divided into three distinct categories: fruits, plants, and crop versus weed. These categories encompass a vast range of agricultural issues and tasks, from the detection and classification of fruits to the identification and differentiation of crops and weeds, all tasks of high relevance in the precision agriculture realm. The fruit category alone included a variety of fruits such as strawberries, mangoes, apples, avocados, rockmelons, and oranges, which represent a wide array of morphological, textural, and color characteristics. The plant category spanned early-stage cotton plants, velvet leaf, tomato plants, and black nightshade plants, providing a diverse set of images with varying complexities. The crop versus weed category provided spatial views of various field scenarios, including carrot plants and weeds, onion plants and weeds, and early-stage corn fields with weeds, all crucial for effective weed management. These datasets were accessed ensuring a comprehensive and diverse sample of real-world agricultural conditions reported by a research survey entitled "A survey of public datasets for computer vision tasks in precision agriculture" by Yuzhen Lu and Sierra Young [66].

2.2 Overview of DALL·E 2 Model

DALL·E 2, an advanced text-to-image generative model developed by OpenAI, serves as a remarkable testament to the intersections of Natural Language Processing and Computer Vision. It leverages the power of hierarchical text-conditional image generation to produce images based on textual descriptions. With a structure founded on two major components - the prior and the decoder - DALL·E 2 employs a sophisticated approach to convert text to visual content. The workflow of the DALL·E 2 model begins with a textual input which is then encoded into a Compact Language-Image Pretrained (CLIP) text embedding via a neural network trained on hundreds of millions of

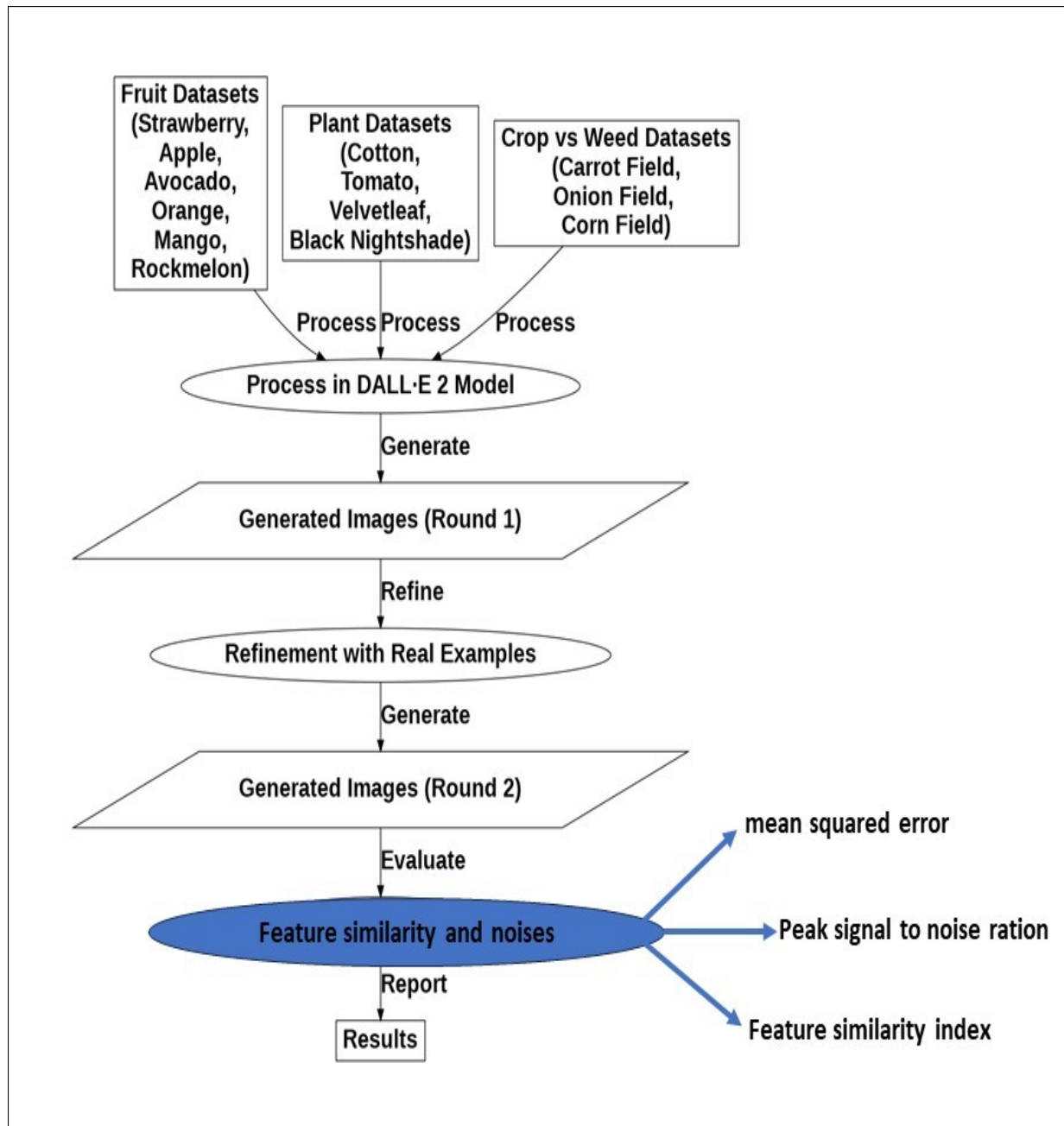


Figure 2: This flowchart illustrates the study's workflow, which involves categorizing datasets, using these to generate initial images with the DALL-E 2 Model, refining these outputs by incorporating original images, and finally producing high-quality, refined images

image-text pairs. The resulting CLIP text embedding undergoes dimensionality reduction through Principal Component Analysis (PCA) before entering the prior stage. Here, a Transformer model with attention mechanism transforms the reduced CLIP text embedding into an image embedding. Following this, the decoder stage, also known as the unCLIP phase, comes into play. A diffusion model Generative Adversarial Network (GAN) takes the image embedding and converts it into an image. The output is subsequently passed through two Convolutional Neural Networks (CNNs) for upscaling: first from 64x64 resolution to 256x256, and then to a final resolution of 1024x1024. According to the recently published blog posts, DALL-E 2 exhibits exceptional capabilities in generating a variety of images from a single textual description, creating original image compositions from semantic components, handling inpainting tasks,

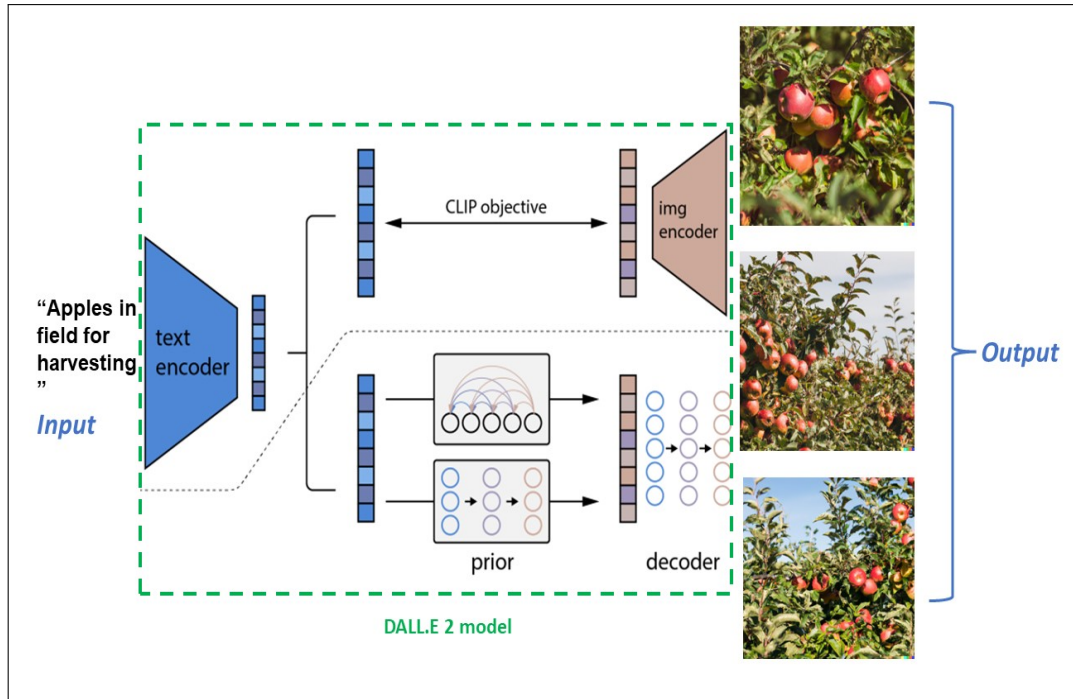


Figure 3: Example of DALL.E 2 image generation using text prompt "Apples in field for harvesting"

and altering images based on subtle changes in the input text. Despite these striking feats, DALL-E 2, like any machine learning model, is constrained by its training data and cannot extrapolate beyond the information it was trained on. Nonetheless, it stands as a significant step forward in AI-driven artistry and design, as well as a powerful tool for visual content generation.

2.3 Text Prompt Creation

In this study, a crucial step was the generation of synthetic images from textual descriptions via the DALL-E 2 model. Covering a comprehensive range of agricultural scenarios was a prime objective, thus careful attention was dedicated to designing the text prompts to mirror these scenarios accurately across the categories: fruits, plants, and crop versus weed. The aim was to guide the AI model, devoid of any pre-loaded examples in its default setting, to create images that visually depicted a broad range of agricultural conditions. The crafting of these prompts focused on their precision, encapsulating diverse elements like stages of plant growth, different times of fruit harvesting, and the differentiation between crops and weeds.

For the fruit category, the inclusion of the term "harvesting" in the prompts was instrumental in directing the AI model towards generating images that were of significant relevance to harvesting-related research. On the other hand, prompts for the plant category consistently incorporated the terms "plants" or "leaf", along with the phrase "early stage", signifying the initial growth stage of the plants. This specification was aimed at aiding research into early detection of potential threats such as pests or diseases. The intention of considering of these strategic elements in prompt selection (Table 1) was to create images that could not only represent these diverse scenarios accurately, but also contribute to the study of various agricultural phenomena and problems.

In meeting the condition of "data with a purpose," the carefully curated text prompts was designed with a specific agricultural context in mind to ensure that the synthetic images generated hold direct relevance to real-world agricultural scenarios. This implies that the resultant data are not merely randomly generated images but hold significant informational value tailored to distinct aspects of agriculture. Whether providing visual representations of various plant growth stages, diverse conditions in fruit harvesting, or distinguishing between crops and weeds, the data generated serves targeted agricultural purposes. Therefore, the synthetic data created isn't superfluous; rather, it's aimed at yielding actionable insights, informing decisions, and possibly shaping interventions within agricultural contexts. This methodical and purposeful approach to data generation is strongly intended with the "data with a purpose" principle, furthering the cause of precision agriculture.

Dataset Type	Prompt
Fruit Datasets	"Strawberries in field for harvesting", "Mangoes in field for harvesting", "Apples in field for harvesting", "Avocados in field for harvesting", "Rockmelons in field for harvesting", "Oranges in field for harvesting"
Plant Datasets	"Early stage cotton plants", "Early stage velvet leaf", "Early stage tomato plant", "Early stage black nightshade plants"
Crop vs Weed Datasets	"Spatial view of carrot plants and weeds in a field", "Spatial view of onion plants and weeds in a field", "Early stage corn field with weed"

Table 2: Text prompts used for different types of datasets in the study

2.4 Generation of Initial Synthetic Images

With the purpose-driven text prompts detailed in Table 1, the initial phase of synthetic image generation was initiated. Each prompt was input into the DALL·E 2 model, inducing the production of a set of four images relevant to the descriptive text. The time taken by the model to generate these four image outputs from each prompt was meticulously recorded, providing a measure of the system's response time. Further, for the purposes of subsequent analysis and evaluation, these sets of synthetic images were preserved. This initial synthetic image generation stage laid the foundation for the ensuing phases of the study, offering a baseline of AI-produced images aligned with targeted agricultural scenarios.

2.5 Iterative Enhancement of Synthetic Images

The succeeding stage in this study involved an iterative refinement process for the initially produced synthetic images. To implement this, one representative example was selected for each textual prompt, sourced from the diverse datasets featured in the "A survey of public datasets for computer vision tasks in precision agriculture" paper referenced previously. These example images were then input into the DALL·E 2 model, which leverages a built-in "generate variations" function. This function empowers the model to predict similar scenarios and generate a variety of realistic images based on the initial input. Thus, through this iterative process, a richer, more diverse set of synthetic images was cultivated, extending the depth and breadth of the original image dataset, and enhancing the realism and applicability of the AI-generated imagery.

2.6 Evaluation Measures

The primary objective of this study was to systematically evaluate the synthetic images generated by the DALL·E 2 model. Two types of synthetic images were considered: those produced solely from textual prompts and those created with the aid of a single image example. Each of these AI-generated images was subjected to an evaluation process against the corresponding original image. This comparison provided objective insights into the quality and realism of the generated images. This process was instrumental in obtaining objective insights into the quality and realism of the AI-generated images.

The evaluation measures utilized in this study are as follows:

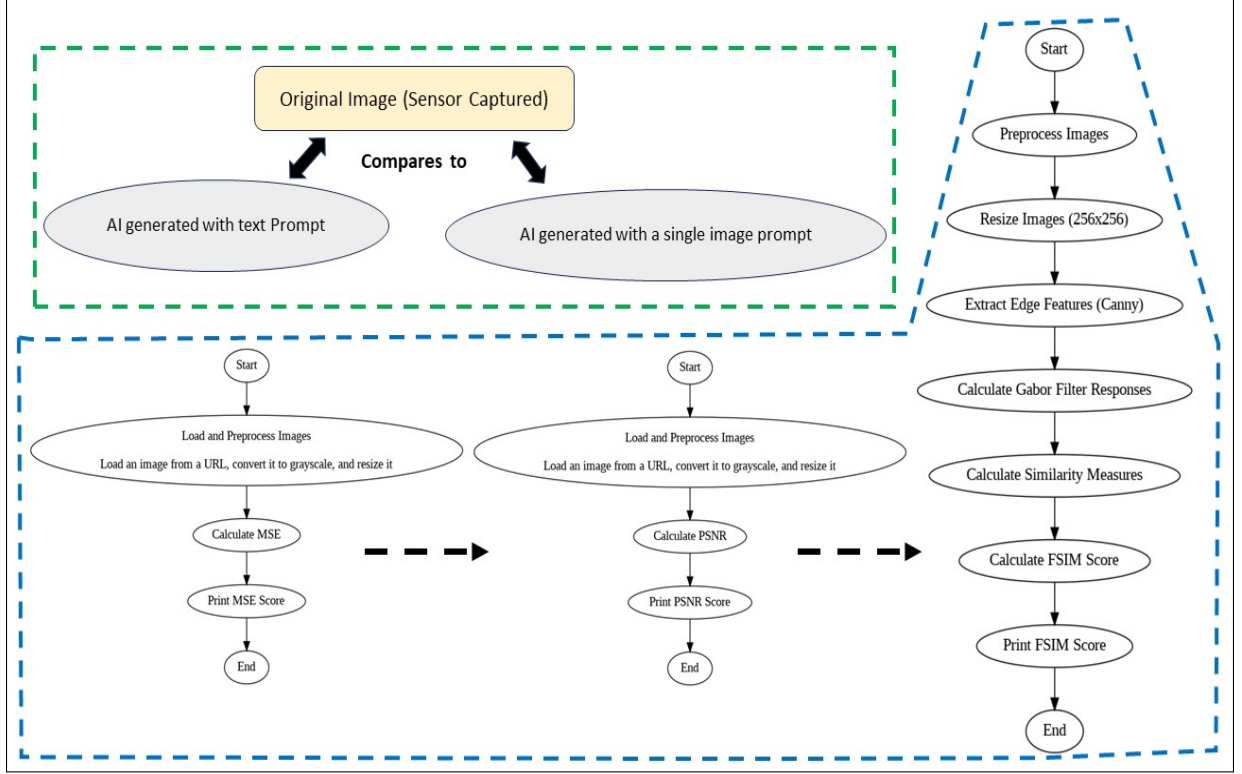


Figure 4: Image analysis procedure

1. **Mean Squared Error (MSE):** MSE quantitatively measures the pixel-level differences between the AI-generated images (G) and the original images (O). It is calculated as the average of the squared differences between corresponding pixels in the two images. Mathematically, MSE is defined as:

$$MSE = \frac{1}{N} \sum_{i=1}^N (O_i - G_i)^2 \quad (1)$$

where N represents the total number of pixels in the images.

2. **Peak Signal to Noise Ratio (PSNR):** PSNR serves as an image quality assessment measure by evaluating the ratio between the maximum possible power of a signal and the power of noise that affects the fidelity of its representation. It is computed using the MSE value as follows:

$$PSNR = 10 \log_{10} \left(\frac{MAX_I^2}{MSE} \right) \quad (2)$$

where MAX_I denotes the maximum possible pixel value of the image.

3. **Feature Similarity Index (FSIM):** FSIM assesses the similarity between the AI-generated images and the original images based on distinct image features. It takes into account both low-level and high-level features, providing a comprehensive measure of similarity. The exact calculation of FSIM involves various comparison functions and their weighted combination, which is beyond the scope of this explanation. However, FSIM is designed to capture the structural, luminance, and contrast information of the images, enabling a more comprehensive evaluation. Mathematically, the calculation of FSIM can be represented as:

$$FSIM = \prod_{k=1}^K \left(\frac{l_k \cdot c_k \cdot s_k}{L_k \cdot C_k \cdot S_k} \right)^{\alpha_k} \quad (3)$$

where l_k , c_k , and s_k are the local similarity, contrast, and structure measurements at scale k , respectively. L_k , C_k , and S_k represent the maximum values of the corresponding measurements, and α_k is the weight assigned to each scale.

The specific equations for calculating l_k , c_k , and s_k involve comparing feature maps, such as gradient maps and structure similarity maps, at different scales. These feature maps capture the characteristics of the images and contribute to the overall FSIM calculation.

In addition to these, an unbiased survey involving agricultural researchers and professionals provided subjective ratings of the images on a 5-point Likelihood Scale. With 1 representing 'Not at all realistic' and 5 being 'Extremely realistic', this survey served to supplement the objective analysis with a subjective perspective, creating a balanced, comprehensive evaluation of the synthetic images.

3 Results

3.1 Image generation only with text prompts

The capacity of the DALL-E 2 model to generate convincing synthetic images without any visual example is truly compelling in agricultural settings. Figure 5 showcases a series of AI-generated images, derived from a variety of textual prompts relating to different fruits in their in-field conditions. Remarkably, these illustrations, achieved with a single shot and devoid of any prior visual input, bear a striking resemblance to their real-world counterparts. The visual synthesis of these fruit datasets, including strawberries, mangoes, apples, avocados, capsicums, rockmelons, and oranges, demonstrates a significant degree of realism. The intricacies of the fruit forms and their placement in what appears to be natural settings, not only establishes the promising capabilities of the model but also opens up a wealth of opportunities for the agricultural automation industry. The potential application of these synthetic images in facilitating image-based research and product development could indeed be a game-changer in the field.

In parallel with the fruitful outcomes derived from the fruit datasets, the DALL-E 2 model exhibited an impressive performance in generating synthetic images pertinent to crop identification. As depicted in Figure 6, the generated representations of early-stage cotton, tomato, velvet leaf, and black nightshade plants manifest the model's prowess in faithfully interpreting the textual prompts to render visually coherent outcomes. Shifting the focus to the more complex domain of crop-weed differentiation, as demonstrated in Figure 7, the model's outputs vary in terms of relevance and accuracy. While the model fell short in producing a relevant aerial image of a carrot field infested with weeds (Figure 7a), it excelled remarkably in the case of the onion field (Figure 7b) and somehow significant view in corn vs weed field (Figure 7c). This disparity in performance underlines the challenges and opportunities inherent to such an AI-driven approach. Despite these variations, the generated images, derived devoid of any initial visual examples, resonate with a high degree of promise, indicating the potential applicability of the DALL-E 2 model in various application side of precision agriculture.

While the initial image generation through textual prompts exhibited substantial potential, some crucial nuances were absent from the resultant synthetic images. An evident illustration of this shortfall was the omission of fruit stems in various images, as exemplified in Figure 9. Key illustrations include synthetic depictions of 'mangoes in field' and 'avocados in field for harvesting', where a multitude of fruits appeared to be suspended in the environment devoid of any connecting stems. This notable absence could pose a significant hurdle for research or applications intending to study the nuances of fruit stems or develop automated harvesting techniques. For instance, initiatives aimed at studying the impact of stem size on fruit health, developing precise fruit-picking robots, investigating stem diseases, exploring the effects of stem thickness on fruit longevity, or assessing the relationship between stem length and ease of fruit harvesting could face considerable challenges due to this shortcoming.

In an exploratory attempt to surmount this issue, a modified approach to synthetic image generation was adopted. The model was re-prompted with revised textual descriptions, such as "Mangoes in field for harvesting with fruits and stem visible on tree", in contrast to the initial, less detailed prompts. This nuanced refinement in the textual input resulted in a more precise representation of the targeted agricultural scenario, where fruits were depicted with their corresponding stems. This iteration effectively exemplifies the adaptability of the DALL-E 2 model and underscores its potential to generate more realistic and accurate synthetic images through more elaborate textual prompts. Such advancements can significantly improve the quality and applicability of AI-generated images with just some textual prompts as an input to the model, thereby making a meaningful contribution to precision agriculture.

3.2 Enhanced Image Generation with Single Example Refinement

The further extension of our study involved the provision of a single real-world RGB image to the DALL-E 2 model as an example, corresponding to each dataset. This step was undertaken with an anticipation to gauge the model's ability to refine its output and hence enhance the realism of the generated images. Preliminary observations suggest that the inclusion of a single real example from the domain during the generation process imparts a significant improvement in



Figure 5: AI-generated images for various fruit datasets without any examples given to the DALL-E 2 model.

the quality and relevance of the synthetic images, thereby further augmenting the model's utility in agricultural domain applications.

In the enhanced image generation process, a single real-world RGB image was provided as an example to the DALL-E 2 model for each dataset, resulting in the generation of variations and refinements. Figure 8 depicts the generated images using the single image input as an example. The first image in each fruit class represents the original image used to train the model, while the subsequent images showcase the generated variations. The images exhibit diverse positions, orientations, and variations of fruits in different locations, offering valuable data for fruit detection algorithms and reducing the need for extensive field data collection. The generated images demonstrate great promise for applications such as harvesting and other agricultural tasks. Notably, the inclusion of the example image during the refinement process significantly improved the similarity and reduced noise, resulting in more realistic and appropriate results.

Similarly, Figure 9 illustrates the results for the plant dataset. In Figure 9b and 9c, the DALL-E 2 model successfully regenerated rows of cotton plants at different locations, showcasing variations in plant structure. Additionally, Figure 9e and 9f highlight the accurate reproduction of the yellowish coloration present in the given input, which was regenerated in different spots. These findings demonstrate the potential of AI-generated images in various agricultural applications, including disease detection models and color analysis for tomato plants during early stages. The generated images exhibit high realism, making them valuable for training and analysis purposes. The same level of authenticity is observed in the images generated using a single example of velvet leaf and black nightshade, indicating their utility across multiple agricultural analyses.



Figure 6: AI-generated images for various plants using simple textual prompts in DALL-E 2 model.

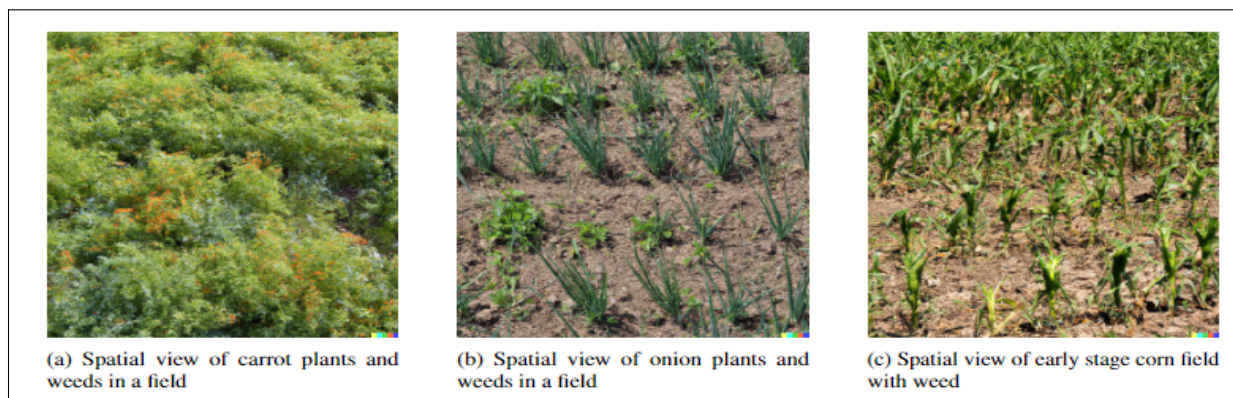


Figure 7: AI-generated images for crop vs weed condition using simple textual prompts in DALL-E 2 model.

The enhanced image generation process, incorporating a single example image, showcases the DALL-E 2 model's adaptability and its ability to generate images that closely resemble real-world agricultural scenarios. These AI-

generated images offer a cost-effective and time-efficient alternative to collecting extensive RGB image data in the field. By utilizing these synthetic images, various agricultural applications can benefit from improved accuracy, realism, and applicability. The results obtained through the enhanced refinement process emphasize the potential of the DALL-E 2 model in advancing precision agriculture and fostering innovative solutions for the agricultural industry.

The evaluation of Mean Squared Error (MSE) scores of the text prompt based AI-generated images from fruit, plant, and crop versus weed datasets revealed variations in accuracy. In the fruit dataset, avocados showed the lowest MSE score (0.096), implying a greater resemblance to original images and a better potential for applications like fruit quality assessment. Conversely, oranges had the highest MSE score (0.15), indicating potential limitations in precise reproduction of the fruit. The plant dataset demonstrated similar patterns; cotton plants scored the lowest MSE score (0.045), while both Velvet leaf and black nightshade showed the highest (0.093). In the crop versus weed dataset, the carrot field images had the lowest MSE score (0.045), while the cornfield images scored highest (0.091). These variations may influence the effectiveness of AI in agricultural applications, including disease detection, plant growth monitoring, and weed management.

Peak Signal-to-Noise Ratio (PSNR) scores also varied across the datasets, providing insights into image quality. In the fruit dataset, rockmelon had the highest PSNR score (15), indicative of superior image fidelity, suitable for applications requiring precise fruit characterization. On the contrary, apple images had the lowest score (8.8), implying potential limitations in capturing fine details. A similar pattern was observed in the plant dataset, with cotton plants achieving the highest PSNR score (19) and tomato plants the lowest (11). In the crop versus weed dataset, carrot and onion fields had the highest PSNR scores (14), while the cornfield scored the lowest (11). These scores hold importance in practical agricultural applications such as plant disease diagnosis, weed detection, and crop yield estimation.

The Feature Similarity Index (FSIM) scores, evaluating the structural similarity between AI-generated and original images, showed variability as well. In the fruit dataset, mango images had the highest FSIM score (0.3), indicating a closer structural resemblance and greater potential for applications like fruit shape recognition. Conversely, rockmelon had the lowest score (0.28), suggesting possible limitations in capturing structural details. The plant dataset showed tomato plant images with the highest FSIM score (0.3) and black nightshade with the lowest (0.25). Finally, in the crop versus weed dataset, the onion field had the highest FSIM score (0.34), while the carrot field and cornfield tied for the lowest (0.33). These scores are crucial in agricultural tasks such as species identification, leaf shape analysis, and weed detection, which rely on accurate structural details.

The application of a single image example to the DALL-E 2 model resulted in modifications in the Mean Squared Error (MSE) scores across diverse datasets. In the fruit dataset, apples exhibited the highest MSE score of 0.13, implying larger deviations from the original, impacting precise applications such as fruit quality assessment. On the contrary, rockmelon achieved the lowest MSE score (0.35), indicating a superior resemblance to the original images. When considering the plant dataset, tomato plants reported the highest MSE score (0.078) potentially affecting tasks like plant disease diagnosis, while cotton plants had the lowest (0.011), promising accurate results in tasks like plant counting. In the crop versus weed dataset, cornfields had the highest MSE score (0.079), suggesting challenges in crop-weed differentiation, whereas the onion field had the lowest score (0.041), indicating accurate representation of field characteristics, enhancing tasks like weed detection. Changes were also observed in the Peak Signal-to-Noise Ratio (PSNR) scores when an image-trained approach was applied. In the fruit category, rockmelon showed the highest PSNR score (15), indicating higher image fidelity suitable for precise fruit characterization, while apple recorded the lowest (8.8), suggesting limitations in capturing details. In the plant dataset, cotton plants registered the highest PSNR score (19), promising accuracy in plant health assessments, whereas tomato plants had the lowest (11), possibly affecting tasks like disease identification. The crop versus weed dataset showed carrot and onion fields with the highest PSNR scores (14), and the cornfield with the lowest (11), affecting the reliability of crop-weed differentiation and yield mapping in cornfields. The Feature Similarity Index (FSIM) scores underwent variations as well with the image-trained approach. In the fruit dataset, orange and mango had the highest FSIM scores (0.29), implying stronger structural similarity, while strawberry had the lowest (0.21), suggesting limitations in capturing structural details. In the plant dataset, tomato plants achieved the highest FSIM score (0.32), hinting at a closer match in structural features, while black nightshade had the lowest (0.23), indicating challenges in capturing fine structural details. Lastly, the crop versus weed dataset reported the onion field with the highest FSIM score (0.34) promising accurate weed identification, whereas the carrot field had the lowest (0.32), indicating challenges in capturing image details affecting tasks like crop-weed differentiation. These variations in MSE, PSNR, and FSIM scores after incorporating image examples indicate DALL-E 2 model's capability to refine its output, underscoring the potential of AI in agricultural applications.

Through these scores, professionals and researchers in the agricultural field can glean a comprehensive understanding of the potential strengths and limitations of AI-generated images, both from text prompts and image input examples. When evaluating AI-generated images based on textual prompts, the significance of these scores cannot be overstated. For instance, a lower MSE score such as those observed in avocados, cotton plants, or onion fields, suggests a high



Figure 8: Variations in DALL-E 2 generated images for different fruits. Subfigures (1), (6), (11), (16), (21) and (26) represent the original images, while subfigures (2)-(5), (7)-(10), (12)-(15), (17)-(20), (22)-(25), and (26)-(30) represent the AI-generated images for strawberries, mangoes, apples, avocados, oranges, and rockmelons, respectively.

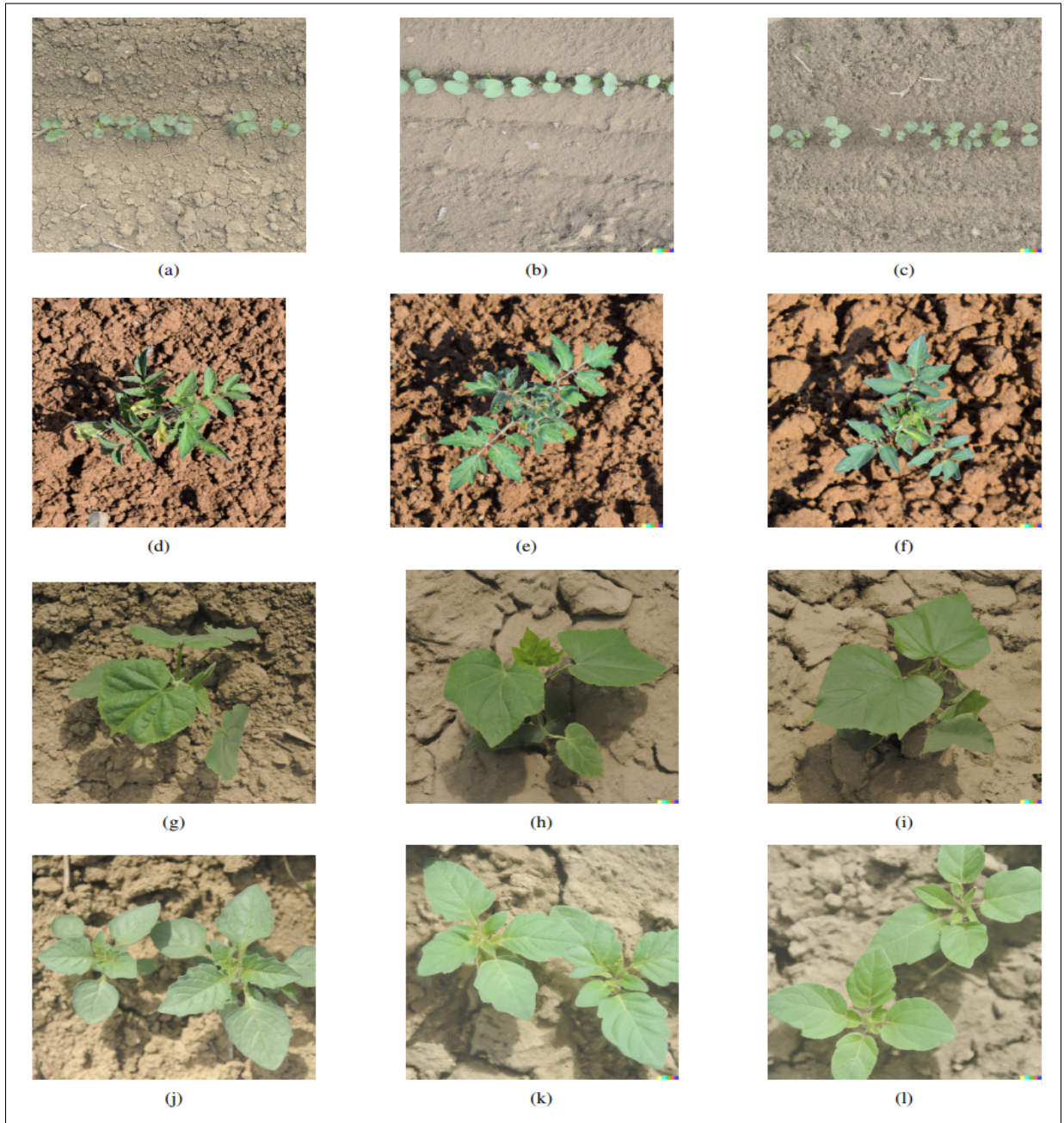


Figure 9: Comparative display of original and DALL-E 2 generated images for different plant categories. Subfigures (a), (d), (g), and (j) represent the original images, while subfigures (b), (c), (e), (f), (h), (i), (k), and (l) represent the AI-generated images. Specifically, subfigures (a)-(c) represent "early-stage cotton plants", subfigures (d)-(f) depict early-stage tomato plants", subfigures (g)-(i) illustrate early stage velvet leaf", and subfigures (j)-(l) portray "early stage black nightshade plants".

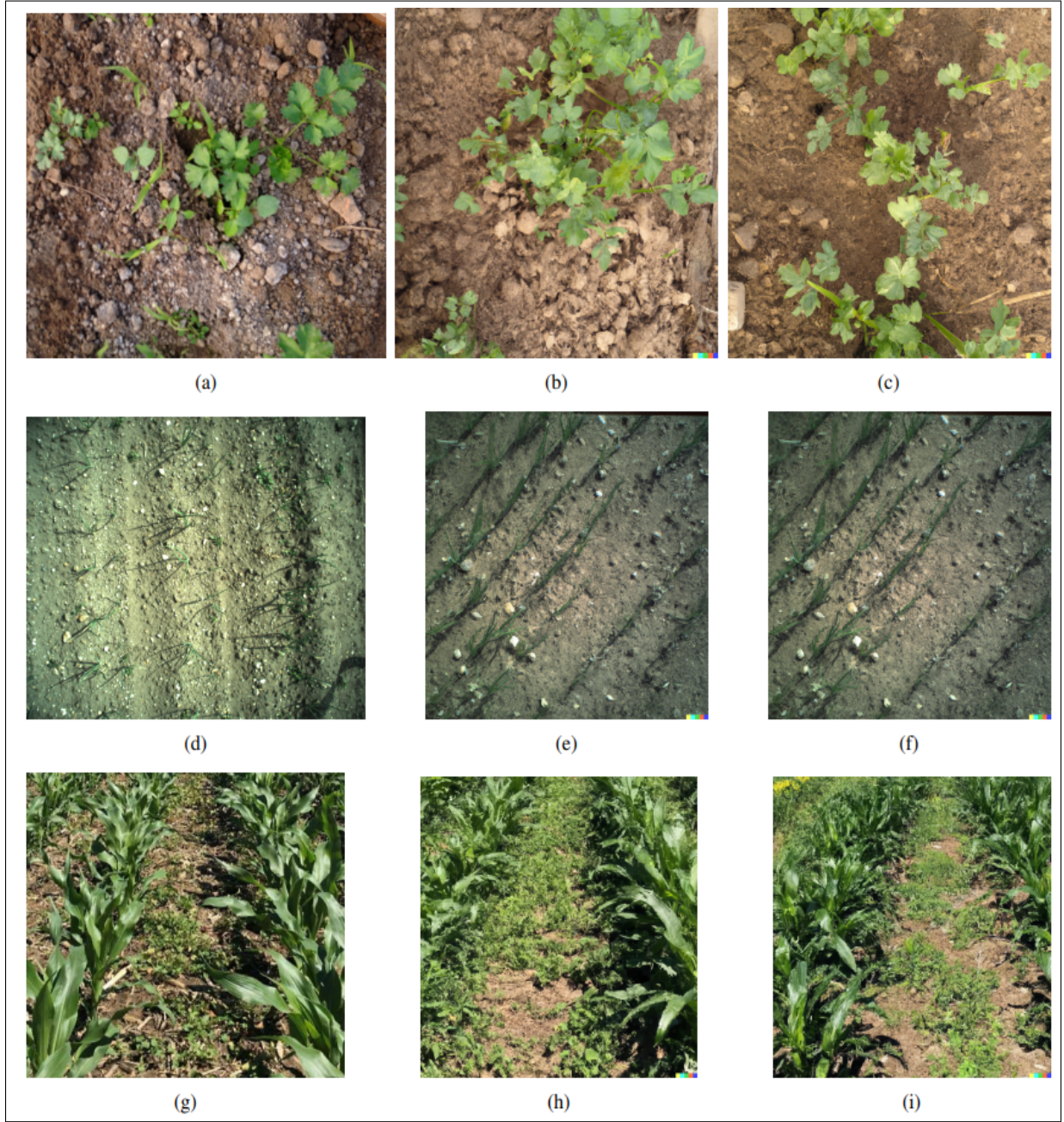


Figure 10: Comparative display of original and DALL-E 2 generated images for different crop versus weed scenarios. Subfigures (a), (d), and (g) represent the original images, while subfigures (b), (c), (e), (f), (h), and (i) represent the AI-generated images. Specifically, subfigures (a)-(c) represent "spatial view of carrot plants and weeds in a field", subfigures (d)-(f) depict "spatial view of onion plants and weeds in a field", and subfigures (g)-(i) illustrate "early stage corn field with weed".

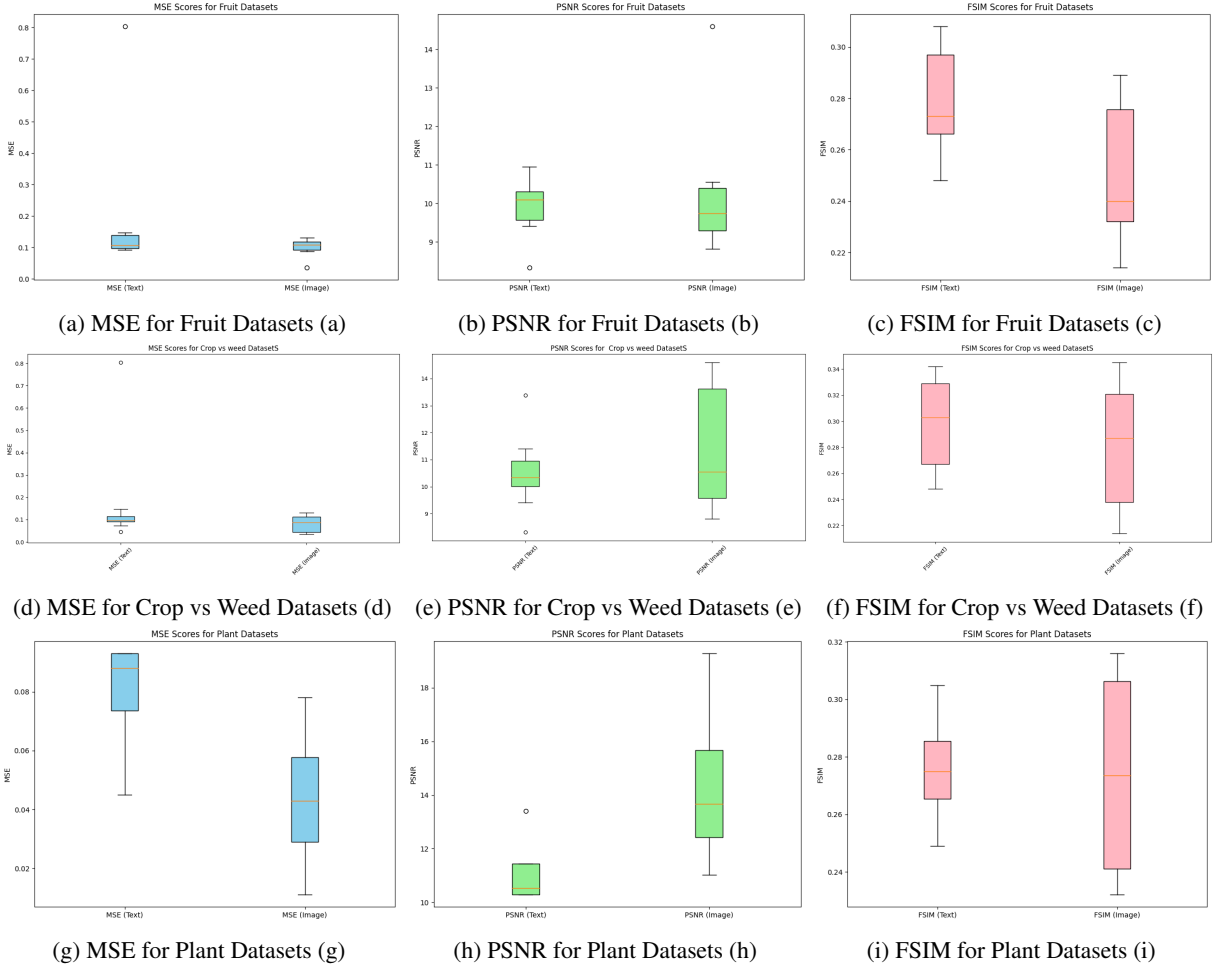


Figure 11: MSE, PSNR, and FSIM Measures : (a) (b) and (c) for fruits dataset, (d) (e) and (f) for plant dataset, and (g) (h) (i) for crop vs weed dataset

level of precision and similarity to the original images. This precision is indispensable for applications like fruit quality assessment and automated harvesting, where accurate representation of agricultural produce is critical for informed decision-making and analysis.

The PSNR score offers another lens to evaluate image quality and clarity, particularly important when image examples are not provided. As observed in rockmelons and cotton plants, a higher PSNR score denotes superior image clarity with less noise. This clarity is crucial for applications demanding detailed observation, such as disease detection and growth monitoring, thereby facilitating improved decision-making and management practices in the agriculture sector.

Assessing structural resemblance between AI-generated images and original images is where the FSIM score becomes crucial. Images of mango or tomato plants with higher FSIM scores depict a closer resemblance in structural features, making them valuable for tasks relying on shape recognition, such as fruit classification and leaf morphology analysis.

From the perspective of both text prompts and image example inputs, these scores offer invaluable insights to stakeholders in agriculture. The measures give an understanding of the capabilities and limitations of AI models like DALL-E 2 in generating images, thereby informing decisions related to various agricultural tasks like crop management, disease detection, and yield estimation. By comprehending the potential of AI-generated images and their alignment with given inputs, stakeholders can strategically leverage these technologies to enhance agricultural productivity, efficiency, and improve decision-making processes. The potential of AI-generated images, as evidenced by the application of the DALL-E 2 model, could revolutionize the way researchers and developers approach image analysis in agriculture. Traditional methods, as demonstrated in numerous recent studies, require extensive data collection from real field scenarios, a process that is time-consuming, labor-intensive, and expensive. These studies, including those focused on

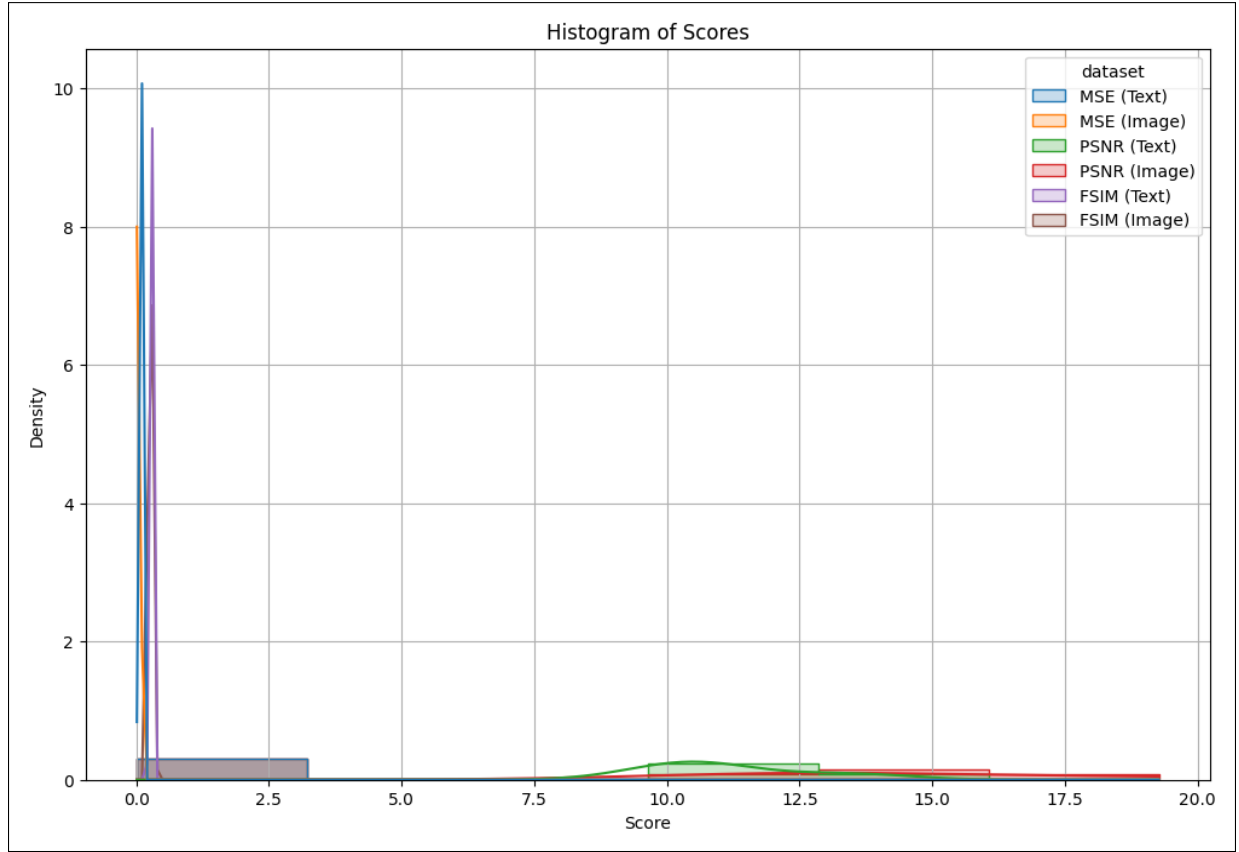


Figure 12: Performance Evaluation of AI Models across Crop Datasets. This histogram depicts the normalized density of Mean Squared Error (MSE), Peak Signal-to-Noise Ratio (PSNR), and Feature Similarity Index Measure (FSIM) scores for two AI models, "Text" and "Image", across 13 crop types. The distribution provides a comparative analysis of the model performance on these diverse datasets.

fruit-related investigations [67, 68, 69, 70, 71], have necessitated countless hours of image collection through various imaging sensors. Similarly, research aimed at weed control applications [72, 73, 74] have expended significant resources collecting field images. Additionally, studies performing early-stage plant disease detection and health monitoring [75, 76] have also been reliant on extensive fieldwork and costly sensor technology for image acquisition.

This study, however, posits an innovative alternative to these traditional, exhaustive approaches. By leveraging the capabilities of AI, specifically through the DALL-E 2 model, synthetic images replicating real field conditions can be generated without the requirement for physical data collection. This process not only significantly reduces the time and labor commitment typically associated with image-based agricultural studies but also minimizes the financial burden linked to sensor technology and field work. It is important to note that the images generated using this method are based on RGB data, aligning with standard image data collection methods in agricultural research. This breakthrough marks a significant stride in agricultural research methodology, demonstrating how AI can transform and streamline existing practices, thereby expanding the possibilities for future exploration and innovation in the field.

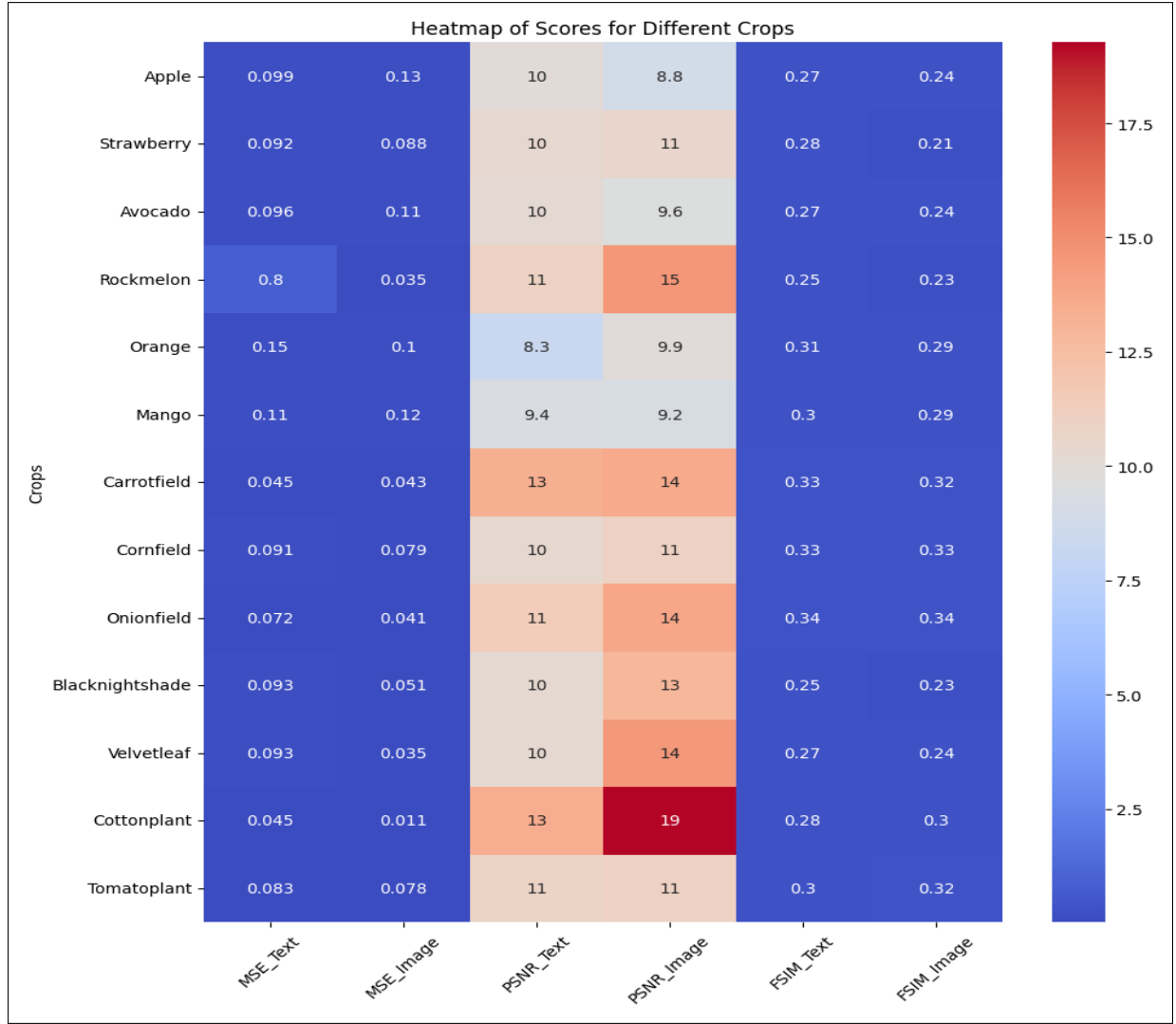


Figure 13: This heatmap visualizes the performance metrics of AI models across 13 different crop types. The color gradients facilitate easy identification of the models' effectiveness, with warmer colors signifying higher values of the Mean Squared Error (MSE), Peak Signal-to-Noise Ratio (PSNR), and Feature Similarity Index Measure (FSIM)

4 Conclusion and future suggestions

This study developed an understanding of the potential of AI-generated images in the agricultural sector. By illustrating the capabilities of DALL·E 2, it demonstrates how the model can generate accurate and realistic synthetic images, which hold considerable promise for various applications in agriculture. Pursuing advancements in evaluation metrics and techniques, expanding and diversifying the training dataset, and enhancing refinement methods all serve to fuel the development of robust AI solutions. By embracing the integration of AI models like DALL·E 2 with existing agricultural systems, the study shines a light on a future where precision agriculture is propelled by the power of AI, heralding a new era of efficiency, accuracy, and innovation in the field. The of AI to generate images based on text prompts and single image examples has paved the way for realistically accurate visuals, offering ground-breaking solutions for tasks such as fruit quality assessment, automated harvesting, disease identification, plant growth monitoring, and crop-weed differentiation. By engaging with this innovative AI model, this research illuminates the path towards a new paradigm in precision agriculture, proposing a sophisticated, technologically-enhanced approach that could drastically change the face of the industry.

This study also indicates the roadmap for the evolution and broader adoption of the DALL·E 2 model in future agricultural settings, suggesting a five-fold approach:

- **Dataset Expansion:** A more extensive set of image examples, encapsulating a wide variety of plant species, diseases, and environmental conditions, could significantly enhance the model’s versatility and the accuracy of the generated images.
- **Advanced Training Techniques:** Leveraging sophisticated training techniques could further refine the model’s learning capability, resulting in a marked improvement in the realism of the image generation process.
- **User Feedback Incorporation:** By integrating feedback from agricultural experts and end users, the model can be continuously optimized. Such insights into the model’s practical applicability and the accuracy of AI-generated images could help in refining the system.
- **Utilization of Diverse Evaluation Metrics:** While this study applied MSE, PSNR, and FSIM for evaluation, considering other metrics, such as the Inception Score (IS), could offer a more rounded evaluation of the AI-generated images’ quality and diversity.
- **Integration with Existing Agricultural Systems:** Encouraging the harmonious integration of AI models like DALL-E 2 with existing agricultural systems can catalyze wider adoption and validate their practical utility in real-world scenarios

References

- [1] John R Schott, Scott D Brown, Rolando V Raqueno, Harry N Gross, and Gary Robinson. An advanced synthetic image generation model and its application to multi/hyperspectral algorithm development. *Canadian Journal of Remote Sensing*, 25(2):99–111, 1999.
- [2] Keith Man and Javean Chahl. A review of synthetic image data and its use in computer vision. *Journal of Imaging*, 8(11):310, 2022.
- [3] Abeer Aljohani and Nawaf Alharbe. Generating synthetic images for healthcare with novel deep pix2pix gan. *Electronics*, 11(21):3470, 2022.
- [4] Richard J Chen, Ming Y Lu, Tiffany Y Chen, Drew FK Williamson, and Faisal Mahmood. Synthetic data in machine learning for medicine and healthcare. *Nature Biomedical Engineering*, 5(6):493–497, 2021.
- [5] Kevin Barrera, Anna Merino, Angel Molina, and José Rodellar. Automatic generation of artificial images of leukocytes and leukemic cells using generative adversarial networks (syntheticcellgan). *Computer methods and programs in biomedicine*, 229:107314, 2023.
- [6] Ildar Lomov and Ilya Makarov. Generative models for fashion industry using deep neural networks. In *2019 2nd International Conference on Computer Applications & Information Security (ICCAIS)*, pages 1–6. IEEE, 2019.
- [7] InMoon Choi, Soonchan Park, and Jiyoung Park. Generating and modifying high resolution fashion model image using stylegan. In *2022 13th International Conference on Information and Communication Technology Convergence (ICTC)*, pages 1536–1538. IEEE, 2022.
- [8] Amit H Bermano, Rinon Gal, Yuval Alaluf, Ron Mokady, Yotam Nitzan, Omer Tov, Oren Patashnik, and Daniel Cohen-Or. State-of-the-art in the architecture, methods and applications of stylegan. In *Computer Graphics Forum*, volume 41, pages 591–611. Wiley Online Library, 2022.
- [9] Xuerong Xiao, Swetava Ganguli, and Vipul Pandey. Vae-info-cgan: generating synthetic images by combining pixel-level and feature-level geospatial conditional inputs. In *Proceedings of the 13th ACM SIGSPATIAL International Workshop on Computational Transportation Science*, pages 1–10, 2020.
- [10] Chong Luo, Yiang Wang, Xinle Zhang, Wenqi Zhang, and Huanjun Liu. Spatial prediction of soil organic matter content using multiyear synthetic images and partitioning algorithms. *Catena*, 211:106023, 2022.
- [11] Isabel Rio-Torto, Ana Teresa Campaniço, António Pereira, Luís F Teixeira, and Vítor Filipe. Automatic quality inspection in the automotive industry: a hierarchical approach using simulated data. In *2021 IEEE 8th International Conference on Industrial Engineering and Applications (ICIEA)*, pages 342–347. IEEE, 2021.
- [12] Yu Guo, Yuxu Lu, and Ryan Wen Liu. Lightweight deep network-enabled real-time low-visibility enhancement for promoting vessel detection in maritime video surveillance. *The Journal of Navigation*, 75(1):230–250, 2022.
- [13] Suncheng Xiang, Dahong Qian, Mengyuan Guan, Binjie Yan, Ting Liu, Yuzhuo Fu, and Guanjie You. Less is more: Learning from synthetic data with fine-grained attributes for person re-identification. *ACM Transactions on Multimedia Computing, Communications and Applications*, 19(5s):1–20, 2023.
- [14] Alain Chen, Liming Wu, Shuo Han, Paul Salama, Kenneth W Dunn, and Edward J Delp. Three dimensional synthetic non-ellipsoidal nuclei volume generation using bezier curves. In *2021 IEEE 18th International Symposium on Biomedical Imaging (ISBI)*, pages 961–965. IEEE, 2021.

- [15] Alberto Álvarez-Trejo, Enrique Cuan-Urquizo, Armando Roman-Flores, LG Trapaga-Martinez, and JM Alvarado-Orozco. Bézier-based metamaterials: Synthesis, mechanics and additive manufacturing. *Materials & Design*, 199:109412, 2021.
- [16] Jordy Davelaar and Zoltán Haiman. Self-lensing flares from black hole binaries: General-relativistic ray tracing of black hole binaries. *Physical Review D*, 105(10):103010, 2022.
- [17] Zinan Zhao and Geriletu Bao. Artistic style analysis of root carving visual image based on texture synthesis. *Mobile Information Systems*, 2022, 2022.
- [18] Ben Mildenhall, Peter Hedman, Ricardo Martin-Brualla, Pratul P Srinivasan, and Jonathan T Barron. Nerf in the dark: High dynamic range view synthesis from noisy raw images. In *Proceedings of the IEEE/CVF Conference on Computer Vision and Pattern Recognition*, pages 16190–16199, 2022.
- [19] Peng Dai, Zhuwen Li, Yinda Zhang, Shuaicheng Liu, and Bing Zeng. Pbr-net: Imitating physically based rendering using deep neural network. *IEEE Transactions on Image Processing*, 29:5980–5992, 2020.
- [20] Tomáš Hodaň, Vibhav Vineet, Ran Gal, Emanuel Shalev, Jon Hanzelka, Treb Connell, Pedro Urbina, Sudipta N Sinha, and Brian Guenter. Photorealistic image synthesis for object instance detection. In *2019 IEEE international conference on image processing (ICIP)*, pages 66–70. IEEE, 2019.
- [21] Julia V Velikina, Andrew L Alexander, and Alexey Samsonov. Accelerating mr parameter mapping using sparsity-promoting regularization in parametric dimension. *Magnetic resonance in medicine*, 70(5):1263–1273, 2013.
- [22] Nils Gräbner, Volker Mehrmann, Sarosh Quraishi, Christian Schröder, and Utz von Wagner. Numerical methods for parametric model reduction in the simulation of disk brake squeal. *ZAMM-Journal of Applied Mathematics and Mechanics/Zeitschrift für Angewandte Mathematik und Mechanik*, 96(12):1388–1405, 2016.
- [23] Teresa Araújo, Ana Maria Mendonça, and Aurélio Campilho. Parametric model fitting-based approach for retinal blood vessel caliber estimation in eye fundus images. *PloS one*, 13(4):e0194702, 2018.
- [24] Stavros Diolatzis, Julien Philip, and George Drettakis. Active exploration for neural global illumination of variable scenes. *ACM Transactions on Graphics (TOG)*, 41(5):1–18, 2022.
- [25] Yuanqing Zhang, Jiaming Sun, Xingyi He, Huan Fu, Rongfei Jia, and Xiaowei Zhou. Modeling indirect illumination for inverse rendering. In *Proceedings of the IEEE/CVF Conference on Computer Vision and Pattern Recognition*, pages 18643–18652, 2022.
- [26] Leon Eversberg and Jens Lambrecht. Generating images with physics-based rendering for an industrial object detection task: Realism versus domain randomization. *Sensors*, 21(23):7901, 2021.
- [27] Joel Vidal, Guillem Vallicrosa, Robert Martí, and Marc Barnada. Brickognize: Applying photo-realistic image synthesis for lego bricks recognition with limited data. *Sensors*, 23(4):1898, 2023.
- [28] Antonia Creswell, Tom White, Vincent Dumoulin, Kai Arulkumaran, Biswa Sengupta, and Anil A Bharath. Generative adversarial networks: An overview. *IEEE signal processing magazine*, 35(1):53–65, 2018.
- [29] Changhee Han, Hideaki Hayashi, Leonardo Rundo, Ryosuke Araki, Wataru Shimoda, Shinichi Muramatsu, Yujiro Furukawa, Giancarlo Mauri, and Hideki Nakayama. Gan-based synthetic brain mr image generation. In *2018 IEEE 15th international symposium on biomedical imaging (ISBI 2018)*, pages 734–738. IEEE, 2018.
- [30] Xian Wu, Kun Xu, and Peter Hall. A survey of image synthesis and editing with generative adversarial networks. *Tsinghua Science and Technology*, 22(6):660–674, 2017.
- [31] Brendan Ross and Jesse Cresswell. Tractable density estimation on learned manifolds with conformal embedding flows. *Advances in Neural Information Processing Systems*, 34:26635–26648, 2021.
- [32] Daniel Matuszczyk, Niklas Tschorn, and Frank Weichert. Deep learning based synthetic image generation for defect detection in additive manufacturing industrial environments. In *2022 7th International Conference on Mechanical Engineering and Robotics Research (ICMERR)*, pages 209–218. IEEE, 2022.
- [33] Jiahui Yu, Zhe Lin, Jimei Yang, Xiaohui Shen, Xin Lu, and Thomas S Huang. Generative image inpainting with contextual attention. In *Proceedings of the IEEE conference on computer vision and pattern recognition*, pages 5505–5514, 2018.
- [34] Bin Liu, Cheng Tan, Shuqin Li, Jinrong He, and Hongyan Wang. A data augmentation method based on generative adversarial networks for grape leaf disease identification. *IEEE Access*, 8:102188–102198, 2020.
- [35] Qiang Dai, Xi Cheng, Yan Qiao, and Youhua Zhang. Crop leaf disease image super-resolution and identification with dual attention and topology fusion generative adversarial network. *IEEE Access*, 8:55724–55735, 2020.

- [36] Yuzhen Lu, Dong Chen, Ebenezer Olaniyi, and Yanbo Huang. Generative adversarial networks (gans) for image augmentation in agriculture: A systematic review. *Computers and Electronics in Agriculture*, 200:107208, 2022.
- [37] LG Divyanth, DS Guru, Peeyush Soni, Rajendra Machavaram, Mohammad Nadimi, and Jitendra Paliwal. Image-to-image translation-based data augmentation for improving crop/weed classification models for precision agriculture applications. *Algorithms*, 15(11):401, 2022.
- [38] Amreen Abbas, Sweta Jain, Mahesh Gour, and Swetha Vankudothu. Tomato plant disease detection using transfer learning with c-gan synthetic images. *Computers and Electronics in Agriculture*, 187:106279, 2021.
- [39] Ruud Barth, JMM IJsselmuiden, Jochen Hemming, and Eldert J van Henten. Optimising realism of synthetic agricultural images using cycle generative adversarial networks. In *Proceedings of the IEEE IROS workshop on Agricultural Robotics*, pages 18–22, 2017.
- [40] Chen-Yi Lu, Dan Jeric Arcega Rustia, and Ta-Te Lin. Generative adversarial network based image augmentation for insect pest classification enhancement. *IFAC-PapersOnLine*, 52(30):1–5, 2019.
- [41] Haseeb Nazki, Jaehwan Lee, Sook Yoon, and Dong Sun Park. Image-to-image translation with gan for synthetic data augmentation in plant disease datasets. *Smart Media Journal*, 8(2):46–57, 2019.
- [42] Ruud Barth, Jochen Hemming, and Eldert J Van Henten. Optimising realism of synthetic images using cycle generative adversarial networks for improved part segmentation. *Computers and Electronics in Agriculture*, 173:105378, 2020.
- [43] Ahmed Ali Gomaa and Yasser M Abd El-Latif. Early prediction of plant diseases using cnn and gans. *International Journal of Advanced Computer Science and Applications*, 12(5), 2021.
- [44] Simon L Madsen, Mads Dyrmann, Rasmus N Jørgensen, and Henrik Karstoft. Generating artificial images of plant seedlings using generative adversarial networks. *Biosystems Engineering*, 187:147–159, 2019.
- [45] Fengle Zhu, Mengzhu He, and Zengwei Zheng. Data augmentation using improved cdcgan for plant vigor rating. *Computers and Electronics in Agriculture*, 175:105603, 2020.
- [46] Zane KJ Hartley and Andrew P French. Domain adaptation of synthetic images for wheat head detection. *Plants*, 10(12):2633, 2021.
- [47] Jordan J Bird, Chloe M Barnes, Luis J Manso, Anikó Ekárt, and Diego R Faria. Fruit quality and defect image classification with conditional gan data augmentation. *Scientia Horticulturae*, 293:110684, 2022.
- [48] Snehal Shete, Srikant Srinivasan, and Timothy A Gonsalves. Tasselgan: An application of the generative adversarial model for creating field-based maize tassel data. *Plant Phenomics*, 2020, 2020.
- [49] Zhongyuan Guo, Hong Zheng, Xiaohang Xu, Jianping Ju, Zhaohui Zheng, Changhui You, and Yu Gu. Quality grading of jujubes using composite convolutional neural networks in combination with rgb color space segmentation and deep convolutional generative adversarial networks. *Journal of Food Process Engineering*, 44(2):e13620, 2021.
- [50] Lukas Drees, Laura Verena Junker-Frohn, Jana Kierdorf, and Ribana Roscher. Temporal prediction and evaluation of brassica growth in the field using conditional generative adversarial networks. *Computers and Electronics in Agriculture*, 190:106415, 2021.
- [51] Jana Kierdorf, Immanuel Weber, Anna Kicherer, Laura Zabawa, Lukas Drees, and Ribana Roscher. Behind the leaves: estimation of occluded grapevine berries with conditional generative adversarial networks. *Frontiers in artificial intelligence*, 5:830026, 2022.
- [52] Jamal R Olatunji, GP Redding, CL Rowe, and AR East. Reconstruction of kiwifruit fruit geometry using a cgan trained on a synthetic dataset. *Computers and Electronics in Agriculture*, 177:105699, 2020.
- [53] Enrico Bellocchio, Gabriele Costante, Silvia Cascianelli, Mario Luca Fravolini, and Paolo Valigi. Combining domain adaptation and spatial consistency for unseen fruits counting: a quasi-unsupervised approach. *IEEE Robotics and Automation Letters*, 5(2):1079–1086, 2020.
- [54] Mulham Fawakherji, Ciro Potena, Alberto Pretto, Domenico D Bloisi, and Daniele Nardi. Multi-spectral image synthesis for crop/weed segmentation in precision farming. *Robotics and Autonomous Systems*, 146:103861, 2021.
- [55] Qingmao Zeng, Xinhui Ma, Baoping Cheng, Erxun Zhou, and Wei Pang. Gans-based data augmentation for citrus disease severity detection using deep learning. *IEEE Access*, 8:172882–172891, 2020.
- [56] Changsu Kim, Hyesoo Lee, and Hoekyung Jung. Fruit tree disease classification system using generative adversarial networks. *International Journal of Electrical & Computer Engineering (2088-8708)*, 11(3), 2021.
- [57] Yunong Tian, Guodong Yang, Zhe Wang, En Li, Zize Liang, et al. Detection of apple lesions in orchards based on deep learning methods of cyclegan and yolov3-dense. *Journal of Sensors*, 2019, 2019.

- [58] Quan Huu Cap, Hiroyuki Uga, Satoshi Kagiwada, and Hitoshi Iyatomi. Leafgan: An effective data augmentation method for practical plant disease diagnosis. *IEEE Transactions on Automation Science and Engineering*, 19(2):1258–1267, 2020.
- [59] Muhammad Hassan Maqsood, Rafia Mumtaz, Ihsan Ul Haq, Uferah Shafi, Syed Mohammad Hassan Zaidi, and Maryam Hafeez. Super resolution generative adversarial network (srgans) for wheat stripe rust classification. *Sensors*, 21(23):7903, 2021.
- [60] Luning Bi and Guiping Hu. Improving image-based plant disease classification with generative adversarial network under limited training set. *Frontiers in plant science*, 11:583438, 2020.
- [61] Yafeng Zhao, Zhen Chen, Xuan Gao, Wenlong Song, Qiang Xiong, Junfeng Hu, and Zhichao Zhang. Plant disease detection using generated leaves based on doublegan. *IEEE/ACM Transactions on Computational Biology and Bioinformatics*, 19(3):1817–1826, 2021.
- [62] Bhavana Nerkar and Sanjay Talbar. Cross-dataset learning for performance improvement of leaf disease detection using reinforced generative adversarial networks. *International Journal of Information Technology*, 13(6):2305–2312, 2021.
- [63] Vivek Sharma, Ashish Kumar Tripathi, and Himanshu Mittal. Technological revolutions in smart farming: Current trends, challenges & future directions. *Computers and Electronics in Agriculture*, page 107217, 2022.
- [64] Sayan De, Ishita Bhakta, Santanu Phadikar, and Koushik Majumder. Agricultural image augmentation with generative adversarial networks gans. In *Computational Intelligence in Pattern Recognition: Proceedings of CIPR 2022*, pages 335–344. Springer, 2022.
- [65] Mariam Badr. Unleashing the power of ai: the microsoft and openai partnership. <https://digital.lib.washington.edu/researchworks/handle/1773/49810>, 2023.
- [66] Yuzhen Lu and Sierra Young. A survey of public datasets for computer vision tasks in precision agriculture. *Computers and Electronics in Agriculture*, 178:105760, 2020.
- [67] Anna Kuznetsova, Tatiana Maleva, and Vladimir Soloviev. Using yolov3 algorithm with pre-and post-processing for apple detection in fruit-harvesting robot. *Agronomy*, 10(7):1016, 2020.
- [68] Tiantian Hu, Wenbo Wang, Jinan Gu, Zilin Xia, Jian Zhang, and Bo Wang. Research on apple object detection and localization method based on improved yolox and rgb-d images. *Agronomy*, 13(7):1816, 2023.
- [69] Meili Sun, Liancheng Xu, Rong Luo, Yuqi Lu, and Weikuan Jia. Fast location and recognition of green apple based on rgb-d image. *Frontiers in Plant Science*, 13:864458, 2022.
- [70] Ricardo Manuel Arias Velásquez. Avocado visual selection with convolutional neural networks based on peruvian standards. In *2022 IEEE XXIX International Conference on Electronics, Electrical Engineering and Computing (INTERCON)*, pages 1–4. IEEE, 2022.
- [71] Shumian Chen, Juntao Xiong, Jingmian Jiao, Zhiming Xie, Zhaowei Huo, and Wenxin Hu. Citrus fruits maturity detection in natural environments based on convolutional neural networks and visual saliency map. *Precision Agriculture*, 23(5):1515–1531, 2022.
- [72] Ranjan Sapkota, John Stenger, Michael Ostlie, and Paulo Flores. Towards reducing chemical usage for weed control in agriculture using uas imagery analysis and computer vision techniques. *Scientific Reports*, 13(1):6548, 2023.
- [73] Boyu Ying, Yuancheng Xu, Shuai Zhang, Yinggang Shi, and Li Liu. Weed detection in images of carrot fields based on improved yolo v4. *Traitement du Signal*, 38(2), 2021.
- [74] Ranjan Sapkota and Joao Flores. Using uav imagery and computer vision to support site-specific weed management in corn. In *ASA, CSSA, SSSA International Annual Meeting*. ASA-CSSA-SSSA, 2021.
- [75] Shangpeng Sun, Changying Li, Peng W Chee, Andrew H Paterson, Yu Jiang, Rui Xu, Jon S Robertson, Jeevan Adhikari, and Tariq Shehzad. Three-dimensional photogrammetric mapping of cotton bolls in situ based on point cloud segmentation and clustering. *ISPRS Journal of Photogrammetry and Remote Sensing*, 160:195–207, 2020.
- [76] Naresh K Trivedi, Vinay Gautam, Abhineet Anand, Hani Moaiteq Aljahdali, Santos Gracia Villar, Divya Anand, Nitin Goyal, and Seifedine Kadry. Early detection and classification of tomato leaf disease using high-performance deep neural network. *Sensors*, 21(23):7987, 2021.